

LA-UR 91-3160

LA-UR-91-3160

--20

DE92 002446

Los Alamos National Laboratory is operated by the University of California for the United States Department of Energy under contract W-7405-ENG-36

NOV 03 1991

TITLE: The High-Strain Rate and Spallation Response of Tantalum,
Ta-10W and T-111

AUTHOR(S): G. T. Gray III and A. D. Rollett

SUBMITTED TO: Fall TMS Meeting 1991
Cincinnati, Ohio
October 20-24, 1991

DISCLAIMER

This report was prepared as an account of work sponsored by an agency of the United States Government. Neither the United States Government nor any agency thereof, nor any of their employees, makes any warranty, express or implied, or assumes any legal liability or responsibility for the accuracy, completeness, or usefulness of any information, apparatus, product, or process disclosed, or represents that its use would not infringe privately owned rights. Reference herein to any specific commercial product, process, or service by trade name, trademark, manufacturer, or otherwise does not necessarily constitute or imply its endorsement, recommendation, or favoring by the United States Government or any agency thereof. The views and opinions of authors expressed herein do not necessarily state or reflect those of the United States Government or any agency thereof.

By acceptance of this article, the publisher recognizes that the U.S. Government retains a nonexclusive, royalty-free license to publish or reproduce the published form of this contribution or to allow others to do so, for U.S. Government purposes.

The Los Alamos National Laboratory requests that the publisher identify this article as work performed under the auspices of the U.S. Department of Energy

MASTER

Los Alamos

Los Alamos National Laboratory
Los Alamos, New Mexico 87545

THE HIGH-STRAIN-RATE AND SPALLATION RESPONSE
OF TANTALUM, TA-10W, AND T-111*

George T. Gray III and A.D. Rollett

Materials Science and Technology Division
Los Alamos National Laboratory
Los Alamos, NM 87545

Abstract

The compressive true stress-true strain response of tantalum, Ta-10W, and T-111 were found to depend on the applied strain rate, in the range 0.001 to 7000 s⁻¹. The strain-rate sensitivities of the flow stress of tantalum, Ta-10W, and T-111 at 1% strain are 0.062, 0.031, and 0.024, respectively. The rates of strain hardening in Tantalum, Ta-10W, and T-111 are seen to exhibit differing behavior with increasing strain rate. The calculated average strain-hardening rate in tantalum, θ , for the quasi-static (0.001 s⁻¹) data at 25⁰ C is 2080 MPa / unit strain. The hardening rate at 3000 s⁻¹ at 25⁰ C decreases to 846 MPa / unit strain. Normalizing the work hardening rate in tantalum with the Taylor Factor for a random polycrystal, [θ / (3.07)²], yields work hardening rates of μ / 276 at quasi-static strain rates and μ / 680 at high-rates, assuming a shear modulus of 61 GPa for tantalum at room temperature. While the work hardening of all the tantalum-based materials are similar at quasi-static rates, alloying results in a small reduction in hardening rate. With increasing strain rate, the work hardening rate in tantalum decreases by approximately a factor of two compared to the alloys. Alloying tantalum with substitutional or interstitial elements is thought to result in increased edge dislocation storage and screw dislocation cross-slip due to interactions with the alloying elements at high strain rates. Increasing temperature increases the strain hardening rate at high strain rate in tantalum while decreasing the yield stress. The rate of work hardening increases between room temperature and 498K after which it remains relatively constant. The calculated hardening rate at 1000⁰ C at 3000 s⁻¹ is 1550/ unit strain compared to 846 / unit strain at 298K and the same strain rate. Further systematic experiments are necessary to determine the connections between: 1) work hardening, 2) substructure evolution, 3) interstitial and substitutional content, 4) crystallographic texture, and temperature / strain rate. The spall strength in the three Ta-based materials is seen to decrease with increased alloy content. With decreasing spall strength the fracture mode during spallation is also seen to change from a more ductile transgranular fracture mode in the case of tantalum to cleavage in the two alloys. The decrease in spall strength and change in fracture mode are both thought to be related to the role of alloying on the localization of plastic deformation and/or deformation twinning and its effect on fracture.

* Work performed under the auspices of the U.S. Department of Energy

Introduction

Structure/property relationships of tantalum and tantalum-based alloys continue to attract scientific interest due to their high density, excellent formability, good heat conductivity, good fracture toughness (even at low temperatures), corrosion resistance, and their weldability[1,2]. Over the past four decades, numerous studies have probed the structure/property response of body-centered cubic (bcc) metals, including a large number of investigations of tantalum and tantalum-based alloys[3-17]. Tantalum, like all bcc metals exhibits deformation behavior which is substantially influenced by impurities, temperature, and strain rate[3]. In contrast to face-centered cubic (fcc) metals, such as Cu or Ni, the flow stress in tantalum below 400K increases rapidly[3-11]. This response has been primarily linked to the large frictional stress (Pierels barrier) necessary to generate and move dislocations through the lattice[3]. There is also thought to be an increased resistance to dislocation motion because pre-existing dislocations are firmly locked by condensed atmospheres of interstitials[3]. The effect of interstitials has been additionally linked to the yield point in bcc metals[3]. The deformation behavior of bcc lattices in general is very sensitive to interstitial impurity atoms, although the varied distortion due to differing interstitials in various lattice constant bcc metals results in different effects. Thermal activation analysis of the deformation behavior of iron and tantalum suggest that the temperature dependence of the yield in tantalum is primarily due to lattice effects while in iron impurity effects dominate[10]. In the low-temperature regime ($<0.2 T_m$) many bcc metals also exhibit alloy softening, the failure of the Schmidt Law, the occurrence of "anomalous slip", and the orientation-dependence of the critical resolved shear stress for slip[3].

In addition to the strong temperature dependence of the yield is also the observation that the work-hardening of bcc metals, when corrected for shear modulus and melting temperature, tends to be lower than fcc metals and also temperature dependent[5,18]. The rate of hardening in niobium tested in tension was found to increase rapidly with increasing temperature between 200K, where θ_{II} is nearly zero, to 500K, where θ_{II} approaches the value of the work-hardening rate in Stage II[18]. With increasing temperature the carbon and nitrogen atoms can diffuse sufficiently rapidly to keep up with the glide dislocations, thereby causing repeated dislocation locking and unlocking in response to the applied stress. Only in the case of Stage I hardening in fcc metals, when the hardening is corrected for the change in shear modulus with temperature, is the rate of work-hardening observed to decrease with decreasing temperature. The hardening rate in Stage II for tantalum and niobium single crystals have been measured to be $\sim\mu/600$ compared to values of the order of $\mu/200$ to $\mu/300$ for fcc metals and alloys[5,6]. Measurements on tantalum single crystals between -385 K and 373 K found that the work hardening rate decreased with decreasing temperature, in contrast to fcc metals[10]. This observation is a major difference between bcc and fcc metals where the Stage II hardening rate increases slightly as is expected due to increased difficulty of cross-slip. Given the ease of cross-slip in bcc metals such as tantalum, as evidenced by wavy slip, this observation remains difficult to resolve. Experiments on tantalum have also shown that below ~300 K Stage II hardening is very low or does not exist but that as the temperature increases θ_{II} increases and then saturates at higher temperatures[6]. The number of dislocations stored per unit strain increase in tantalum with decreasing temperature, coincident with the observation of long straight screw dislocations suggesting suppressed cross-slip[9].

In parallel with the rapid increase in flow stress with decreasing temperature, the rate sensitivity of bcc metals is high[3]. The strain-rate sensitivity for tantalum has been measured to be 0.084 at $\dot{\epsilon}=0.1$, 295K, and a strain rate of 10^{-2}s^{-1} and decreasing to 0.03 with increasing strain, $\dot{\epsilon}=0.18$ [14]. In comparison the rate sensitivity of copper was measured to be ~0.014 and relatively independent of strain [14]. Concurrent with the high rate sensitivity in tantalum is a factor of two decrease in the strain hardening exponent from $n=0.27$ at a rate of 10^{-4}s^{-1} to $n=0.13$ at 10^{-2}s^{-1} [14]. Additional studies on tantalum have also revealed a trend for decreasing work hardening with increasing strain rate[15-17]. Work on niobium single crystals has also noted that θ_{II} decreases strongly with increasing strain rate[18]. Temperature variations are seen to have a bimodal influence on the strain hardening of tantalum. At 298K the strain hardening was found to decrease with strain rate ($n=0.27$ and 0.13 at 10^{-4} and 10^{-2}

s^{-1} , respectively) while at 798K the strain hardening exponent remained constant ($n \sim 0.20$) over the strain rate range of 10^{-4} to $10^3 s^{-1}$ [15].

The purpose of this paper is to report the results of a preliminary study of the effect of alloying, strain rate, and temperature on the mechanical behavior of tantalum, Ta-10W, and T-111 and the spallation response of the three Ta-based alloys. The rate sensitivity, work-hardening, and spall strength are discussed and contrasted to literature data on BCC metals in terms of alloying, defect storage, and the substructure evolution.

Experimental Procedures

The materials used for this investigation were commercially-pure arc-melted tantalum (labeled Tantalum "A"), Ta-10W, and T-111 (8W-2Hf) with compositions as listed in Table I. The tantalum, Ta-10W, and T-111 were supplied in 5-mm-thick plate, 5-mm-thick plate, and 25.4-mm-dia. rod, respectively. The tantalum and Ta-10W were received in annealed form while the T-111 was annealed at $1650^{\circ}C$ for 1 hour. The as-tested microstructures of the tantalum, Ta-10W, and T-111 were all equiaxed grains with nominal grain sizes of $45 \mu m$, $60 \mu m$, and $40 \mu m$, respectively.

Table I - Alloy Compositions (in ppm wt. %)

Material	C	N	O	H	Fe	Ni	Cr	W	Hf	Ta
Tantalum*	<40	<40	<100	<10	<50	<50	<50	<150		bal.
Ta -10W*	<30	<35	<100	<10	<50	<50	<50	9-11%		bal.
T-111	85	<10	210	<5	37	<10	<10	9.8%	2.5%	bal.

*nominal compositions

The mechanical responses of the three tantalum-based materials were measured in compression using solid-cylindrical samples 7.6 mm in dia. by 4.6 mm long, lubricated with molybdenum grease. Quasi-static compression tests were conducted on a screw-driven load frame at strain rates of 0.001 and $0.1 s^{-1}$. Dynamic tests, strain rates of $1000-8000 s^{-1}$, were conducted as a function of strain rate and temperature utilizing a Split-Hopkinson Pressure Bar. High temperature tests were performed in a vacuum furnace mounted on the Split-Hopkinson Bar[19]. The high temperature Hopkinson-Bar samples were lubricated with a boron nitride powder / alcohol slurry which was allowed to dry on the sample prior to testing. The inherent oscillations in the dynamic stress-strain curves and the lack of stress equilibrium in the specimens at low strains make the determination of yield inaccurate at high strain rates. Accordingly, the Hopkinson Bar data at strains of less than 1 to 2% are not shown.

The dynamic fracture response of the three tantalum materials under shock-loading was investigated on samples impacted in an 80-mm single-stage launcher. The spall strengths of the samples were measured using manganin gauges positioned behind the sample. All the spallation experiments were conducted using symmetric-material impact conditions to achieve simple-centered flow during the spall and to reduce shock-wave impedance mismatch effects thereby facilitating soft recovery of the samples for subsequent fractographic analysis. The peak shock pressure was controlled by varying the impact velocity of the projectile. The spall strengths were calculated from the magnitude of the "pull-back" signal in the stress-time signal using the bulk shock velocity and the formalism developed by Romanchenko and Stepanov[20]. Details of the experimental procedures utilized in the spallation experiments are given elsewhere[21]. Samples for optical metallography were sectioned from the deformed

samples. The fracture surfaces of the recovered spall samples were examined in a scanning electron microscope (SEM).

Results and Discussion

Stress-Strain Response

The compressive true stress-true strain response of Tantalum, Ta-10W and T-111 were found to depend on the applied strain rate, which ranged from 0.001 to 7000 s⁻¹ (Figures 1-3). The flow stress of tantalum, Ta-10W and T-111 were all seen to increase with increasing strain rate. A summary of the flow stresses at 2% strain for low and high strain rates, measured rate sensitivities, and calculated strain hardening rates at low and high strain rates are listed in Table II. The strain-rate sensitivities, "m" ($= \delta \ln \sigma / \delta \ln \dot{\epsilon}$), of the flow stress of tantalum, Ta-10W, and T-111 at 2% true strain are 0.062, 0.031, and 0.024, respectively. The observation of a rapid increase in yield for all three tantalum materials with increasing strain rate is consistent with a high Peierls stress in BCC metals as documented by previous studies on refractory metals and alloys[3]. The rate-sensitivity is additionally seen to decrease with alloying content which reflects the significantly larger effect of alloying on the low-strain rate flow behavior compared to that at high rate where the inherent large lattice friction dominates. This finding is opposite the effect noted due solely to interstitial content in tantalum where increasing oxygen or nitrogen content was accompanied by an increased hardening rate and an increased rate sensitivity[22].

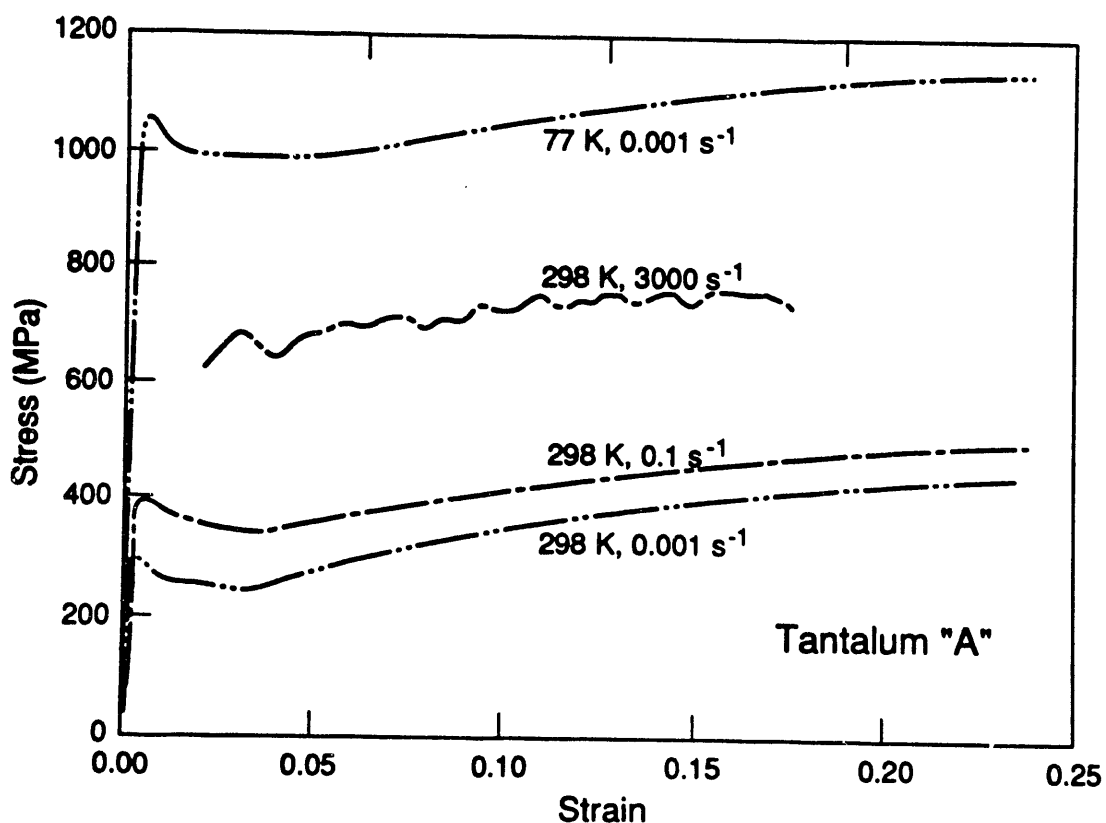
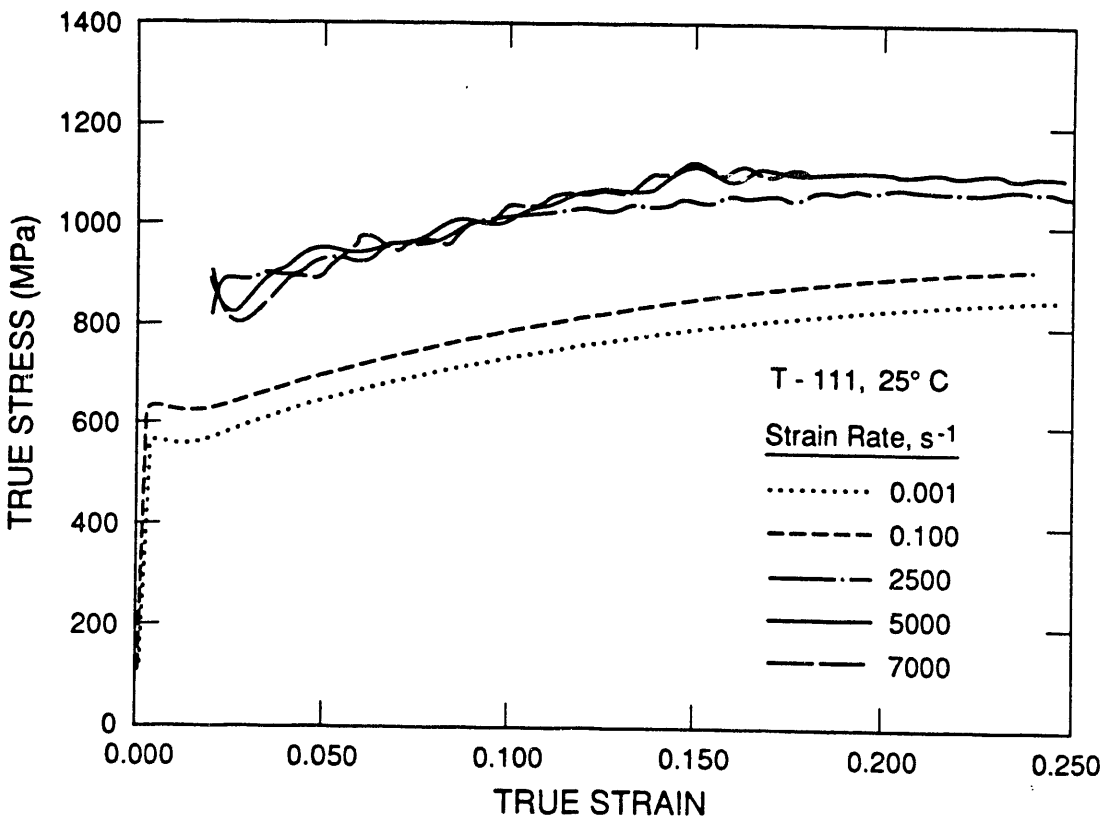
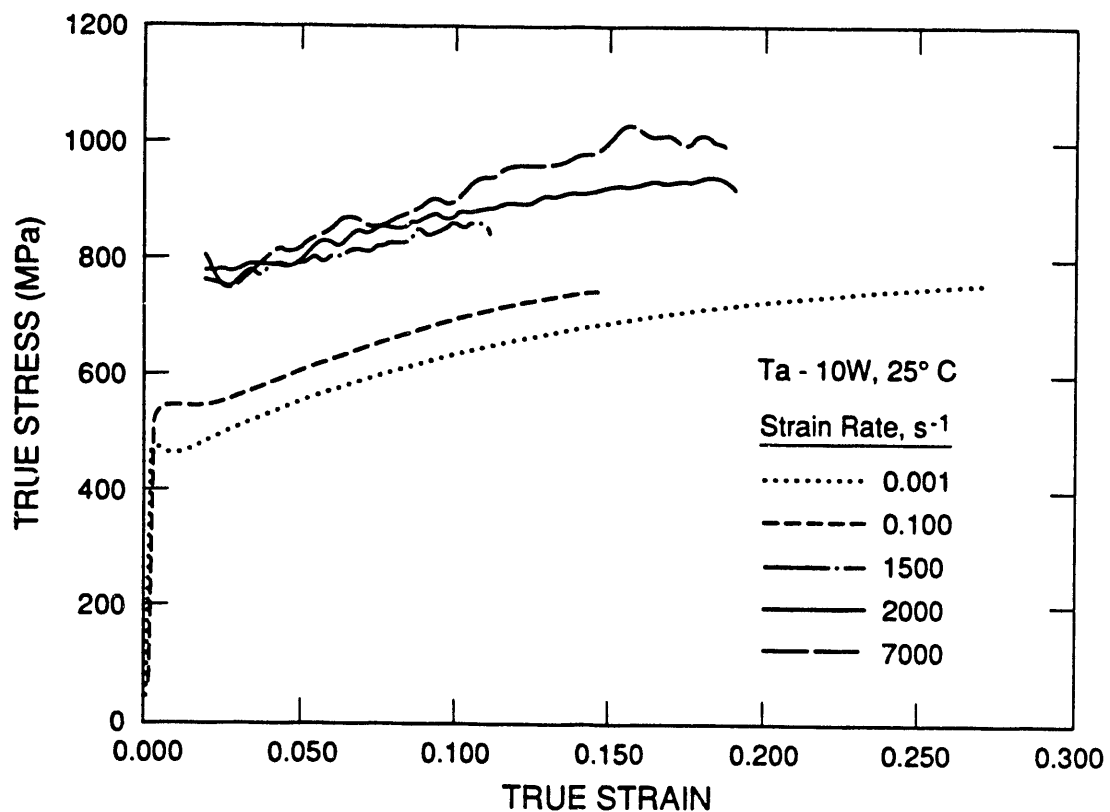


Figure 1 - Compressive Stress-Strain response of Tantalum as a function of the applied strain rate at 25° C. The oscillations in the curve at $\dot{\epsilon} = 3000 \text{ s}^{-1}$ arise from elastic wave motion in the pressure bars and do not reflect true material behavior.



Increasing temperature at high rates is observed to decrease the flow stress of tantalum (Figures 4). The decrease in flow stress with increasing temperature is consistent with previous studies [11,12,15]. Similar to the quasi-static results of Hoge and Mukherjee [11] the flow stress decreases rapidly initially with increasing temperature and then slows its decrease to almost a plateau. Optical metallographic examination of the tantalum samples subsequent to deformation as a function of strain rate and temperature have revealed that while wavy slip predominates, evidence of deformation twins are also observed. A limited number of twins are seen in isolated grains following high-rate straining at room temperature and also following quasi-static deformation at 77 K, particularly following larger strains ($\epsilon > 0.50$). Figure 5 shows evidence of deformation twins in a tantalum sample deformed to a true strain of 0.60 at 77 K quasi-statically. These observations are similar to previous studies which have shown that impact / high-rate loading at 77 K [24] and room temperature [25] can produce deformation twins in tantalum.

Table II - Summary of Stress-Strain Data at 298K as a Function of Strain Rate

Material	$\sigma @ 2\% \epsilon$ (MPa)		$m = \delta \ln \sigma / \delta \ln \dot{\epsilon}$	Strain Hardening Rate "n" (MPa per unit strain)	
	10^{-3} s^{-1}	10^3 s^{-1}		10^{-3} s^{-1}	10^3 s^{-1}
Ta	250	640	0.062	2080	846
Ta-10W	475	775	0.031	2065	1730
T-111	560	825	0.021	1570	1530

The rates of strain hardening in Tantalum, Ta-10W, and T-111 are seen to exhibit differing behavior with increasing strain rate. The calculated average strain-hardening rate in tantalum, θ , for the quasi-static (0.001 s^{-1}) data at 25^0 C is $2080 \text{ MPa / unit strain}$. The hardening rate at 3000 s^{-1} at 25^0 C is reduced to $846 \text{ MPa / unit strain}$. Normalizing the work hardening rate in tantalum with the Taylor Factor for a random polycrystal, [$\theta / (3.07)^2$], yields work hardening rates of $\mu / 276$ for the quasi-static rate data and $\mu / 680$ for the high-rate data assuming a shear modulus of 61 GPa for Ta at room temperature. While the work hardening of all tantalum materials are similar at quasi-static rates, alloying results in a small reduction in hardening rate. With increasing strain rate the work hardening rate in tantalum decreases by approximately a factor of two compared to the alloys. In contrast to the tantalum alloys where the small decrease in strain hardening is probably due to adiabatic heating, the larger decrease in the hardening rate in tantalum at high rate is clearly related to other processes. Similar to studies on pure tantalum where the work-hardening rate decreases significantly with decreasing temperature, increasing strain rate results in decreased defect storage due to restricted screw dislocation motion, i.e. straight screw motion and little new dislocation line generated due to the high Peierls stress. Alloying tantalum with substitutional or interstitial elements appears to result in increased edge dislocation storage and screw dislocation cross-slip due to interactions with the alloying elements at high strain rates.

The strain hardening rate increases with increasing temperature at high strain rate in tantalum. The rate of work hardening increases between room temperature and 498 K after which it remains relatively constant. The hardening rate at 1000^0 C at 3000 s^{-1} is $1550 / \text{unit strain}$ compared to $846 / \text{unit strain}$ at 298 K and the same strain rate. Several studies on tantalum single crystals [6,10] have observed that the rate of Stage II hardening increases with increasing temperature and then saturates at higher temperature. In the work of Arsenault and Lawley [6] this saturation temperature for tantalum was approximately 475 K ; below 300 K , however, Stage II hardening was minimal or absent altogether.

Collectively, the effects of increasing strain rate and temperature result in decreased and increased strain hardening behavior, respectively. This behavior is paradoxical when compared to (typical) fcc materials for which the rate of strain hardening increases with decreasing temperature and increases with increasing strain rate. A previous study of the substructure evolution linked to these trends has shown that at elevated temperatures the dislocation structure consists of primary screw dislocations, dipole clusters, and individual dipoles[6]. At low temperatures, the dipole clusters and individual dipoles are absent. Substructure evaluation on tantalum deformed at high-rate, exhibiting nearly zero hardening at high rate, has also shown a predominance of primary straight screw dislocations[17]. This observation is consistent with the single crystal observations[6] whereas in the present study, the rate of strain hardening decreased with increasing strain rate but did not go to zero. Additional recent results[23] on another lot of commercially-pure tantalum, while showing reduced hardening at high rate ($\sim 4000 \text{ s}^{-1}$ at 298K), also do not exhibit flat stress-strain curves. In these recent tests, however, the samples deformed anisotropically which has subsequently been linked by texture measurements to an anisotropic texture in the plane of the plate investigated. Further systematic experiments are necessary to determine the connections between: 1) work hardening, 2) substructure evolution, 3) interstitial and substitutional content, 4) crystallographic texture, and temperature / strain rate.

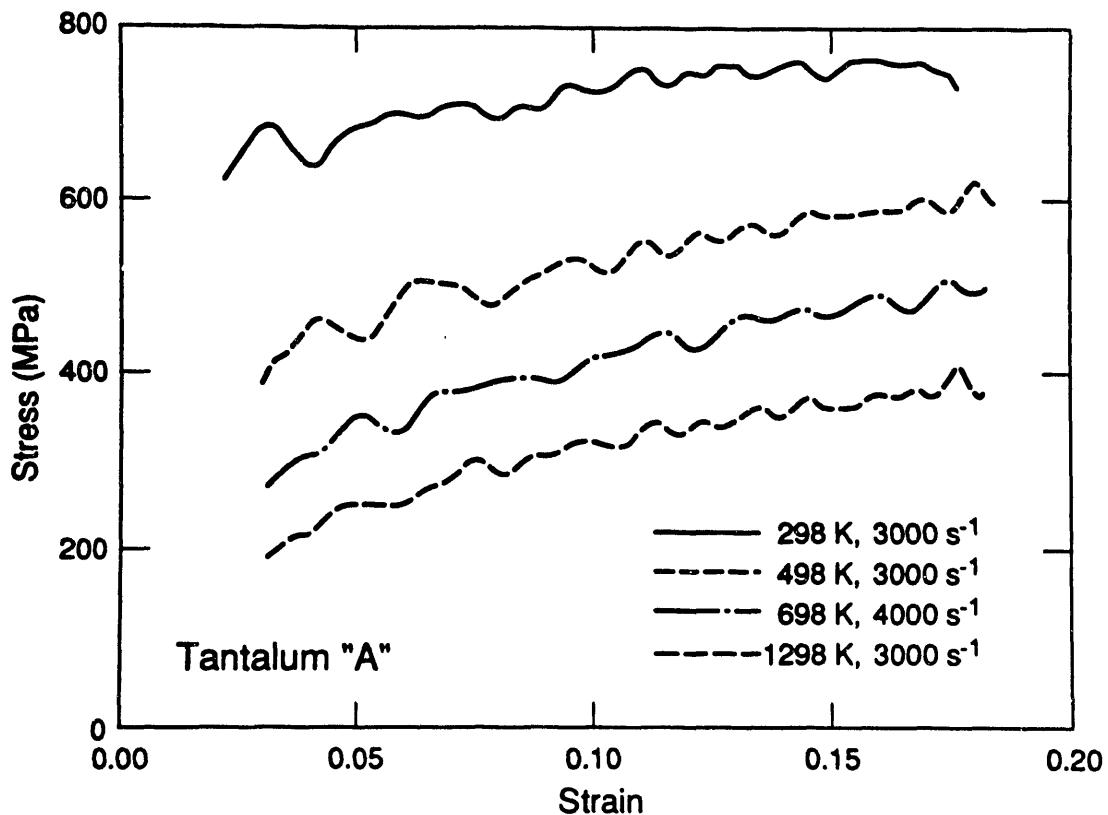


Figure 4 - Compressive stress-strain response of Tantalum as a function of test temperature at a strain rate of $\sim 3000 \text{ s}^{-1}$.

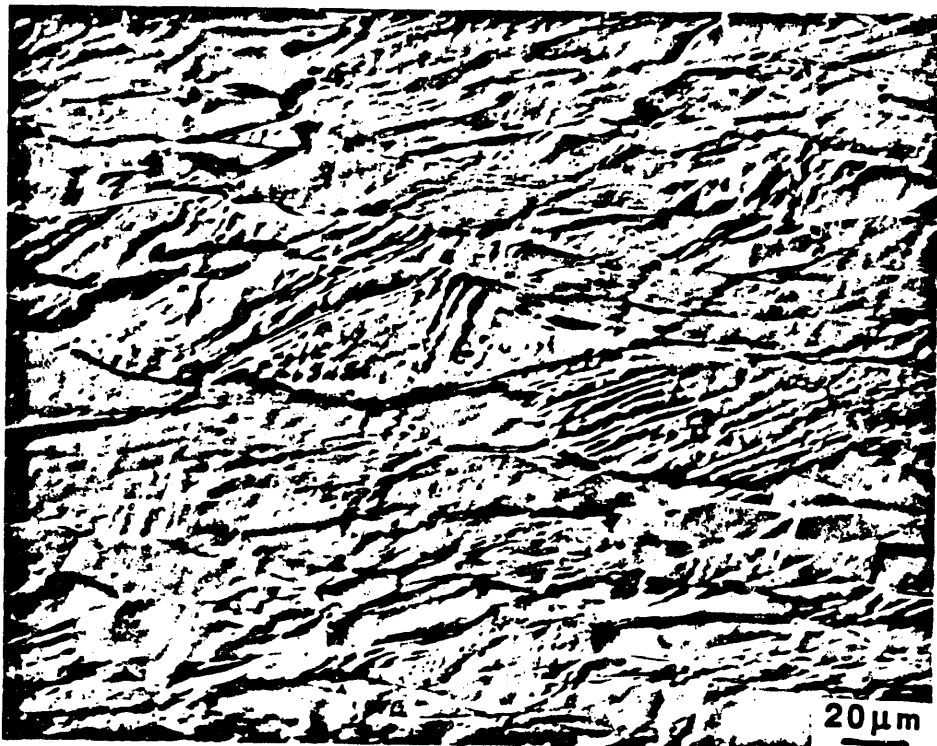


Figure 5 - Optical metallographic photograph of deformation twins in tantalum deformed quasi-statically to a strain of 0.60 at 77 K.

Spall Strength

Table 3 lists the impact conditions and spall data for tantalum, Ta-10W, and T-111. Figure 6 shows an example of one of the stress-time spall traces for tantalum. The deep pull-back signal in this trace reflects the high spall strength (3.7 -4.4 GPa) of tantalum. The spall strength in the three Ta-based materials is seen to decrease with increased alloying. With decreasing spall strength the fracture mode during spallation also changes from a more ductile transgranular fracture mode in the case of tantalum to cleavage in the two alloys.(Figure 7) The decrease in spall strength and change in fracture mode are both thought to be related to the role of alloying on the localization of plastic deformation and its effect of fracture. In Group V_A metals (vanadium, niobium, and tantalum) plastic deformation is characterized by wavy slip under most conditions leading to considerable ductility even at low temperatures. Under severe loading rates and temperatures these metals can however fail in a brittle manner initiated by transgranular cleavage. In this case the cleavage fracture is normally associated with the ductile-to-brittle transition and has often been associated with the observation of significant amounts of deformation twinning. Given the localization of slip into narrow bands which cannot be transmitted into an adjoining grain or a twin impinging on a strong obstacle such as a grain boundary or in particular another twin, large stress concentrations can be generated which will initiate a crack triggering cleavage. In the case of Group VI_A metals (tungsten, chromium, molybdenum) the large susceptibility of these metals to impurity segregation at grain boundaries triggers intergranular fracture and/or cleavage. The observation of high spall strengths associated with high-purity tantalum and lower values for tungsten and molybdenum

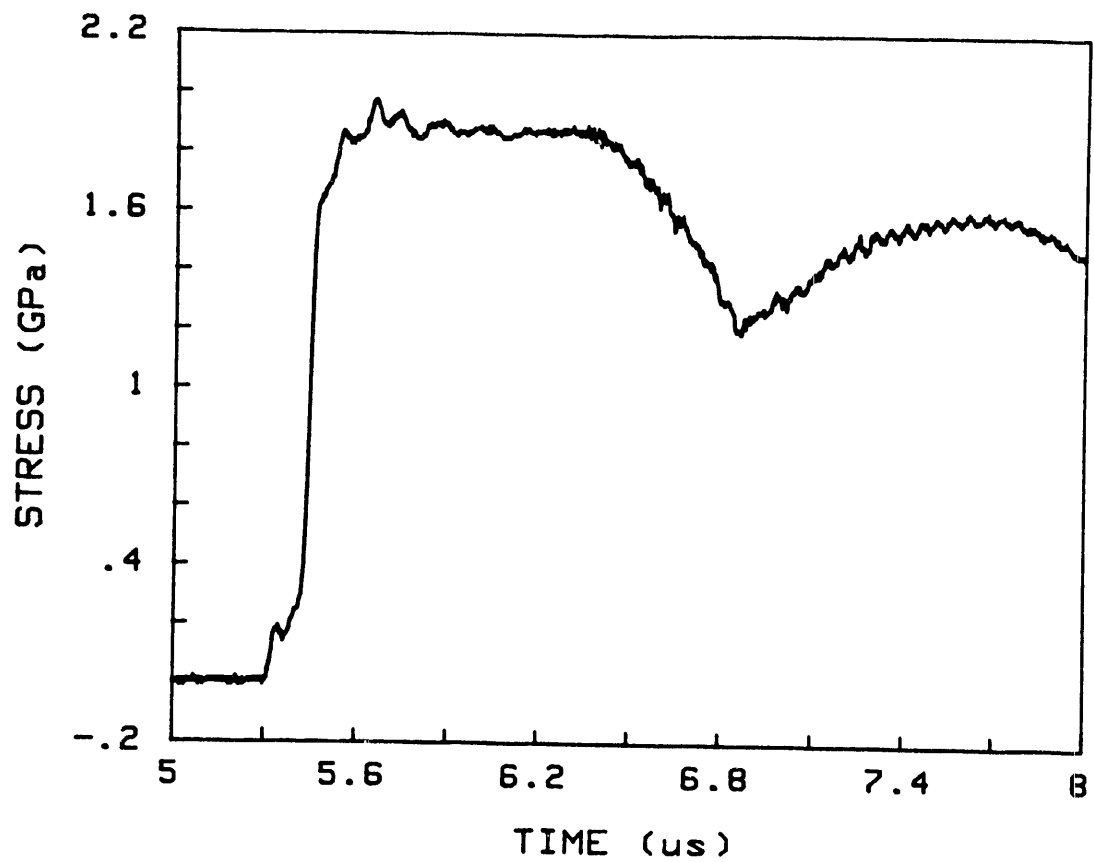


Figure 6 - Stress-Time Spall Trace of Tantalum

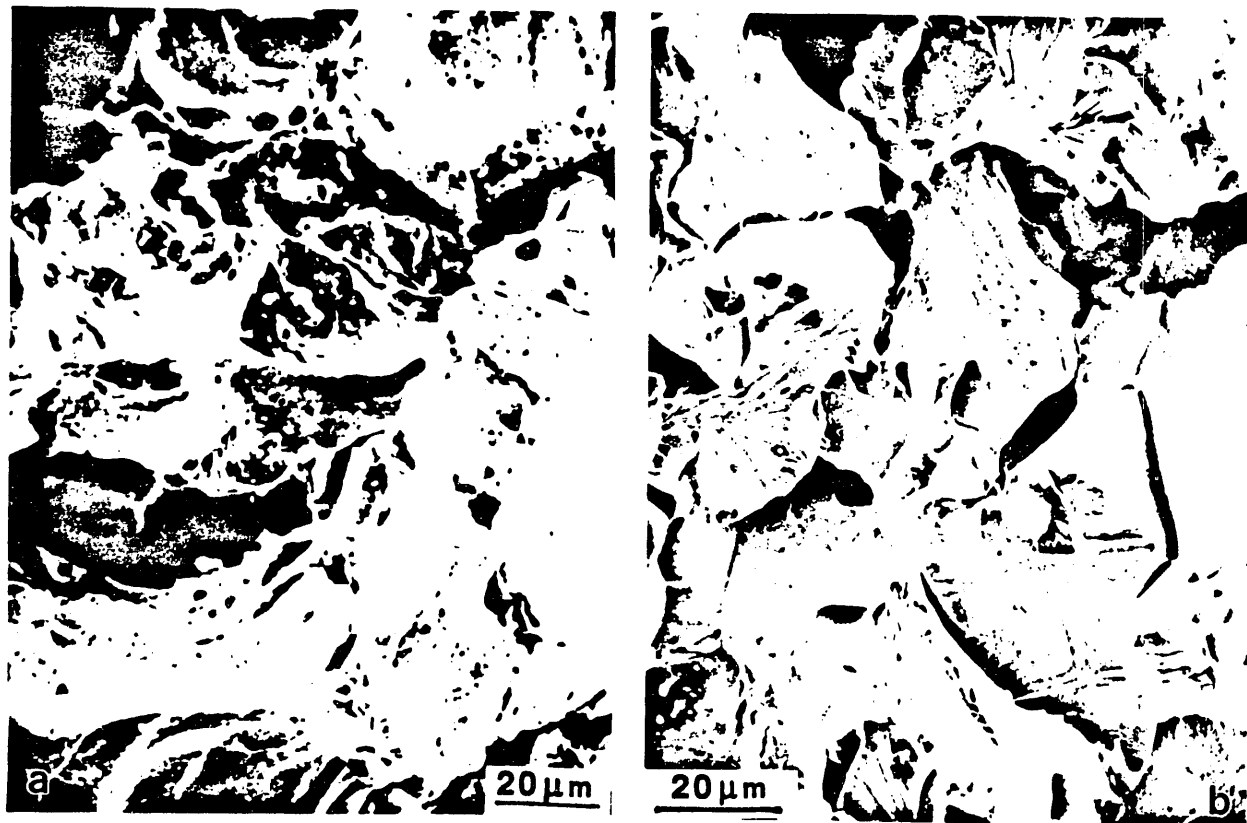


Figure 7 - SEM Micrograph of the Fracture Morphology in Spalled: a) Tantalum. (Note the mixture of cleavage and localized ductile fracture), and b) Ta-10W showing cleavage fracture.

are consistent with the work of Chhabildas[26]. In his studies the spall strength of tantalum was measured to be 3.5 times higher than tungsten[26].

Table 3 - Spall Data

Material	Impact Velocity (m/sec)	Shock Pressure (GPa)	Spall Strength (GPa)	Fracture Character
Tantalum	504	15	4.4	Ductile Transgranular
	503	15	3.7	
Ta-10W	456	14	3.4	Cleavage
	494	15	3.0	
T-111	494	15	3.1	Cleavage

Part of this difference in spall strength (and fracture toughness) can be traced to the difference in elastic / plastic properties between tantalum and tungsten. Tantalum has an anomalously low shear modulus, $G = 61$ GPa, and Young's modulus of 186 GPa whereas tungsten has a high shear modulus of 160 GPa and Young's modulus of 345 GPa[27]. The yield strengths of annealed tantalum and tungsten at room temperature are also very different, $\sigma_w \sim 4 \times \sigma_{Ta}$. Crystals cleave when resistance to plastic shear is so great that at some point (or area) within the crystal the cohesive strength is exceeded. Based on criterion governing the nucleation of slip and dislocation mobility, Ashby has examined several dimensionless groups of material properties that can be used to rank the tendency of metals to fail via cleavage[28]. One of these dimensionless property groups is[28]:

$$z = \frac{(\sigma_{y0})^2 \Omega^{1/3}}{E \gamma} \quad [1]$$

where σ_{y0} = flow stress at 0° K
 Ω = atomic molar volume
 E = Young's modulus
 γ = surface energy.

Utilizing values of the material properties[27] for tantalum [$\sigma_{y0} = 1.5$ GPa, $\Omega = 1.8 \times 10^{-29}$ m³, $E = 186$ GPa, $\gamma = 3.4$ J/m²] and tungsten [$\sigma_{y0} = 3.8$ GPa, $\Omega = 1.6 \times 10^{-29}$ m³, $E = 345$ GPa, $\gamma = 4.2$ J/m²] the dimensionless group value for tantalum gives $z=3.2$ compared to 8.5 for tungsten[28]. This can be compared to $z=0.44$ for copper which does not cleave and $z= \sim 9.9$ for magnesium which readily fractures by cleavage. This material property approach would predict an increased tendency toward cleavage fracture with increasing flow stress as would be the case upon alloying tantalum; consistent with the results of this study.

Microstructurally, a detailed understanding of the role of alloying in tantalum alloys on spall strength depends on an accurate assessment of alloying and impurity effects on slip character, twinning propensity, and fracture initiation under shock-loading conditions. If indeed twinning is the initiator of cleavage fracture in Ta-alloys, the effect of alloying is to raise the flow stress for slip, thus making twinning more likely to occur. As twinning becomes more frequent, more cleavage initiation sites become available, thus causing a transition from

transgranular ductile rupture in unalloyed to cleavage in alloyed tantalum. The decrease in spall strength associated with the transition is appreciable but the alloys are still fracture resistant. In this case the high ductility observed in high-purity tantalum reflects the predominance of slip-controlled plasticity. Further systematic studies are required to ascertain the role of alloying on fracture initiation, including determining the role of deformation twinning and/or localized slip in this process.

Summary and Conclusions

Based on a study of the influence of strain rate and temperature on the stress-strain and spallation response of Tantalum, Ta-10W, and T-111, the following conclusions can be drawn:

1. The compressive true stress-true strain response of Tantalum, Ta-10W, and T-111 were found to depend on the applied strain rate. The strain-rate sensitivities of the flow stress of Tantalum, Ta-10W, and T-111 at 1% strain are 0.062, 0.031, and 0.024, respectively.
2. The rates of strain hardening in Tantalum, Ta-10W, and T-111 are seen to exhibit differing behavior with increasing strain rate. The calculated average strain-hardening rate in tantalum, θ , for the quasi-static (0.001 s^{-1}) data at 250°C is $2080\text{ MPa / unit strain}$. The hardening rate at 3000s^{-1} at 250°C decreases to $846\text{ MPa / unit strain}$. Normalizing the work hardening rate in tantalum with the Taylor Factor for a random polycrystal, $[\theta / (3.07)^2]$, yields work hardening rates of $\mu / 276$ at quasi-static strain rates and $\mu / 680$ at high-rates, assuming a shear modulus of 61 GPa for tantalum at room temperature. Increasing temperature increases the strain hardening rate at high strain rate in tantalum. The rate of work hardening is seen to increase between room temperature and 498K after which it remains relatively constant. The calculated hardening rate at 1000°C at 3000 s^{-1} is $1550/\text{ unit strain}$ compared to $846/\text{ unit strain}$ at 298K and the same strain rate.
3. The spall strength in the three Ta-based materials is seen to decrease with increased alloying. The spall strengths of tantalum, Ta-10W, and T-111 were ~ 4.0 , 3.2 , and 3.1 GPa , respectively. With decreasing spall strength upon alloying, the fracture mode during spallation changes from ductile transgranular fracture in the case of tantalum to cleavage in the two alloys. The decrease in spall strength and change in fracture mode appears related to the role of alloying on the flow stress for slip, localization of plastic deformation and twinning.

Acknowledgments

The authors acknowledge the assistance of M.F. Lopez for conducting the quasi-static compression tests, C. Trujillo for conducting the Hopkinson-Bar tests, and C.E. Frantz for conducting the spall test analysis. The author would like to acknowledge stimulating discussions with J.D. Embury and U.F. Kocks. This work was performed under the auspices of the U.S. Department of Energy.

References

1. W. Kock and P. Paschen, "Tantalum- Processing, Properties and Applications," JOM, 41(10) (1989), 33-39.
2. C. Feng and P. Kumar, "Correlating Microstructure and Texture in Cold-Rolled Ta Ingots," JOM, 41(10) (1989) 40-45.

3. J.W. Christian, "Some Surprising Features of the Plastic Deformation of Body-Centered Cubic Metals and Alloys," Metall. Trans., 14A(1983) 1237-1256.
4. A. Gilbert, D. Hull, W.S. Owen, and C.N. Reid, "The Yield of Polycrystalline Tantalum," J. Less-Common Metals, 4 (1962) 399-408.
5. T.E. Mitchell and W.A. Spitzig, "Work-Hardening in Tantalum Single Crystals," Refractory Metals and Alloys IV, ed. R.I. Jaffee, G.M. Ault, J. Maltz, and M. Semchyshen, (Gordon and Breach, New York, 1967) 25-45.
6. R.J. Arsenault and A. Lawley, "Work-Hardening Characteristics of Ta and Ta-base Alloys," Work Hardening, ed. J.P. Hirth and J. Weertman, (Gordon and Breach, New York, 1968) 283-309.
7. R.L. Smialek and T.E. Mitchell, "Interstitial Solution Hardening in Tantalum Single Crystals," Philos. Mag., 22 (1970) 1105-1127.
8. L.A. Gypen and A. Deruyttere, "Thermally Activated Deformation in Tantalum-Base Solid Solutions," J. Less-Common Metals, 86 (1982) 219-240.
9. D. Hull and W.S. Owen, "The Interaction of Interstitial Solute and Substructure in Refractory Metals," Tungsten, Tantalum, Molybdenum, Niobium, and Their Alloys, ed. N.E. Promisel, (Pergamon Press, Oxford, 1964) 95-109.
10. B.L. Mordike, "Plastic Deformation of Zone Refined Tantalum Single Crystals," Z. Metallkunde, 53 (1962) 586-592.
11. K.G. Hoge and A.K. Mukherjee, "The Temperature and Strain Rate Dependence of the Flow Stress of Tantalum," J. Mat. Sci., 12 (1977), 1666-1672.
12. V.P. Kraschenko and V.E. Statsenko, "Influence of Temperature and Deformation Rate on the Strength of Tantalum / Report 2. Mechanisms and Processes of Occurrence of Plastic Deformation," Problemy Prochnosti, 3 (1981) 60-65.
13. G. Regazzoni, F. Montheillet, R. Dormeaval, and M. Stelly, "Influence of Strain-Rate on the Flow Stress and Ductility of Copper and Tantalum," Deformation of Polycrystals: Mechanisms and Microstructures, ed. N. Hansen, A. Horzewell, T. Leffers, and H. Lilholt, (Riso National Laboratory, Denmark, 1981) 343-349.
14. G. Regazzoni and F. Montheillet, "Influence of Strain Rate on the Flow Stress and Ductility of Copper and Tantalum at Room Temperature," Mechanical Properties at High Rates of Strain, 1984, ed. J. Harding, (Institute of Physics #70, Oxford, 1984) 63-70.
15. J.C. Giannotta, G. Regazzoni, and F. Montheillet, "Ductility and Flow Rule of Tantalum at 20 °C and 500°C," DYMAT 85, (J. de Physique, France, 1985) C5-49-54.
16. W.H. Gourdin, "Constitutive Properties of Copper and Tantalum at High Rates of Tensile Strain: Expanding Ring Results," Mechanical Properties at High Rates of Strain 1989, ed. J. Harding, (Institute of Physics #102, Oxford, 1989) 221-226.
17. D.H. Lassila and G.T. Gray III, "Effects of Shock Prestrain on the Dynamic Mechanical Behavior of Tantalum," DYMAT 91, (J. de Physique, France) in press.
18. T.E. Mitchell, R.A. Foxall, and P.B. Hirsch, "Work-Hardening in Niobium Crystals," Philos. Mag., 8 (1963) 1895-1920.
19. C.E. Frantz, P.S. Follansbee, and W.J. Wright, "New Experimental Techniques with the Kolsky Bar," High Energy Rate Fabrication, ed. I. Berman and J.W. Schroeder, (NY:

Am. Soc. Mech. Engr., 1984), 229.

20. V.I. Romanchenko and G.V. Stepanov, " Dependence of the Critical Stress on the Loading Time Parameters during Spall in Copper, Aluminum, and Steel," Zhur. Prik. Mekh. Tekh. Fiz., 4(1980), 141-147.
21. A.K. Zurek, P.S. Follansbee, and J. Hack, "High Strain-Rate-Induced Cleavage in Mild Carbon Steel," Metall. Trans., 21(1990) 431-439.
22. M.G. Ulitchny and R. Gibala, "The Effects of Interstitial Solute Additions on the Mechanical Properties of Niobium and Tantalum Single Crystals," J. Less-Common Metals, 33 (1973) 105-116.
23. G.T. Gray III, unpublished results, Los Alamos National Laboratory (1991).
24. C.S. Barrett and R. Bakish, "Twinning and Cleavage in Tantalum," Trans. AIME, 212 (1958) 122-123.
25. R.W. Anderson and S.E. Bronisz, "Twining in Tantalum, " Acta Metall., 7 (1959) 645-646.
26. L.C. Chhabildas, L.M. Barker, J.R. Asay, and T.G. Trucano, "Spall Strength Measurements on Shock-Loaded Refractory Metals," Shock Compression of Condensed Matter-1989, ed. S.C. Schmidt, J.N. Johnson, and L.W. Davison, (Elsevier Science Publishers, 1990), 429.
27. H.J. Frost and M.F. Ashby, Deformation-Mechanism Maps, (Oxford, England: Pergamon Press, 1982), 32.
28. M.F. Ashby, private communication, Cambridge University, 1985.

END

DATE
FILMED

12/03/91

